Journal of Theoretical and Applied Information Technology
20th April 2013. Vol. 50 No.2

ISSN: 1992-8645 www.jatit.org E-ISSN: 1817-3195

FIBER GRATING ATMOSPHERIC PRESSURE SENSOR BASED ON MICRO-BENDING CHARACTERISTIC

LUO YINGXIANG
School of Electronics and Information Engineering, Chongqing Three Gorges University, Chongqing, China

ABSTRACT

This paper proposed a new pressure sensor based on long period fiber grating resonant peak modulation through the LPFG microbending sensitivity characteristics and membrane structure with box. Research results show that: the sensor measurement is in the range of 0～0.25 MPa, the detection resolution is 0.24469 hPa/dB, LPFG resonance spectroscopy changing law and the theoretical derivation, numerical analysis results are in good agreement with ANSYS. By appropriate selection of the diaphragm material, packaging structure parameters, which can obtain good corresponding relation and the measurement range, further improving the detection precision, can satisfy the weather and aircraft height measurement of pressure sensor requirements.

Key words: *Long-Period Fiber Grating; Atmospheric Pressure Sensor; Bending; Resonance Peaking Amplitude*

1. INTRODUCTION

Atmospheric pressure measurement is not only an important parameter in the meteorological telemetering system, but also a modern aircraft to realize height measurement, which is one of the important ways. At present, the practical application is often employed in the resonant tube type, capacitance or resistance box film pressure sensor measuring atmospheric pressure [1]. Resonant cylinder pressure transducer has a stable work, small error, high resolution, but with small pressure range, complex structure, high cost, limited application field. In addition, the sensor will stop secretly phenomenon, cause observed failures, and easily affected by environmental factors that occur with aging [2]. Capacitive pressure sensor with high sensitivity, small zero drift, low power consumption advantages, but its high output impedance, load capacity of poor, parasitic capacitance and capacitance on the sensitivity and accuracy of the impact is bigger, the external environment (i.e., temperature, humidity, electrostatic, pollution etc) and output nonlinear will effect. The resistance strain gauge is used for detection of air pressure, and the air pressure sensor performance can be improved, but the effect of temperature and additional stress can be caused by large measurement error.

In order to avoid the above shortcomings, this long period fiber grating technology is introduced into the pressure sensor field, using LPFG on the bending sensitive characteristics, a long period fiber grating (LPFG) and the circular box film structure of the combination. Then constitute a special LPFG- film box package, so it has the anti interference and high sensitivity to ambient pressure changes in the environment, which can be better applied to atmospheric pressure measuring and vehicle height determination. So it has good application prospects.

2. SENSING PRINCIPLE

The germanium-doped single model fiber by the ultraviolet written grating technology forms Fiber Bragg Grating. Its fiber core presents the periodic distribution. When the temperature, strain, stress or other detecting physical around the grating changes, it will lead the grating cycle or the core refractive index changing, then cause Bragg fiber grating wavelength excursion, contrarily monitoring the Bragg fiber grating wavelength excursion using fiber grating demodulator can obtain the changes of detecting physical [3-6], basic principle as shown in Figure 1.

Journal of Theoretical and Applied Information Technology
20th April 2013. Vol. 50 No.2

ISSN: 1992-8645 www.jatit.org E-ISSN: 1817-3195

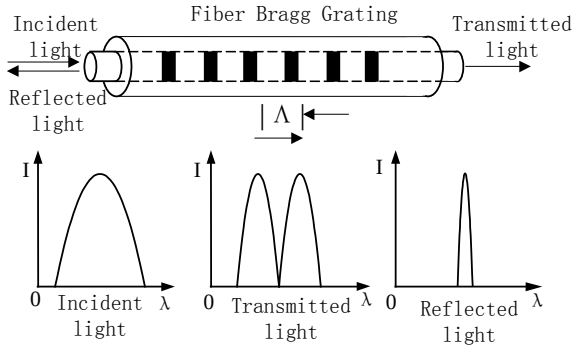

Fig.1 Fiber grating reflection spectrum and transmission spectrum

3. LPFG PRESSURE SENSOR PRINCIPLE AND NUMERICAL ANALYSIS

3.1 LPFG bending properties

When the long period fiber grating (LPFG) is bent, bent on the impact of LPFG occurs mainly in 2 aspects: one is that [3] fiber has curved waveguide; on the other hand is to make LPFG per a modulated refractive index section tilts (relative to the first cycle was modulated refraction in terms of rate of cross section).

Let Λ be not bent LPFG period, R LPFG radius of curvature, the second cycle by modulation of the refractive indices of the cross-section of the tilt angle $\theta = \Lambda / R$, then the i cycle by modulation of the refractive indices of the cross-section of the tilt angle of $\theta_i = \Lambda(i-1)/R$. Equivalent grating in the fiber core refractive index distribution can be expressed as [3] $n_{\text{eff}}^{\text{co}}(z)$:

$$n_{\text{eff}}^{\text{co}}(z) = n_{\text{eff}}^{\text{co}} + \bar{\delta} n_{\text{eff}}^{\text{co}}(z')\left\{1 + \nu \cos\left[\frac{2\pi}{\Lambda_i'} z' + \phi(z')\right]\right\} \quad (1)$$

Type: $z' = x\sin\theta_i + z\cos\theta_i \approx z\cos\theta_i$; $n_{\text{eff}}^{\text{co}}$ is the core of the fiber DC effective refractive index. Grating inclined main effect is to grating fringe visibility and the decrease of ν so that each grating period core average effective refractive index modulation $\bar{\delta} n_{\text{eff}}^{\text{co}}$ is reduced, so that the cross coupling coefficient $k_{kj}(z,\theta)$ decreased, the expression for the [3]

$$k_{kj}(z,\theta) = \frac{\nu_{kj}(\theta)}{2}\sigma(z) \quad (2)$$

Type : $\sigma(z)$ self coupling coefficient, by long period fiber grating coupling rate expressions can be seen, the grating bending will make the equivalent straight LPFG tilt angle increases, the core and cladding mode coupling between the coefficient is reduced, so that the resonant peak amplitude decreased.

Core schemas and in-phase transmission loss peaks normalized bandwidth can be approximated as:

$$\frac{\Delta\lambda}{\lambda} \cong \frac{\lambda}{\Delta n L}\left(1 + \frac{4k_{kj}L}{\pi}\right)^{\frac{1}{2}} \quad (3)$$

Type : λ for approximate resonant wavelength, $\Delta n = n_{\text{eff}}^{\text{co}} - n_{\text{eff}}^{\text{cl}}$ as the core and the cladding mode of the effective refractive index difference. For each of a defined wavelength, long period fiber grating transmission T_λ can be expressed as:

$$T_\lambda = \frac{A^{\text{co}}(L/2)}{A^{\text{co}}(-L/2)} \quad (4)$$

Use of type (4) calculation of curvature on LPFG resonant transmission spectrum influence curve is shown in Figure 2 [7-9], LPFG in the drawing bending respectively is 0 mm,0.75 mm,1.5 mm,2.25 mm,3.0 mm and 3.75 mm.

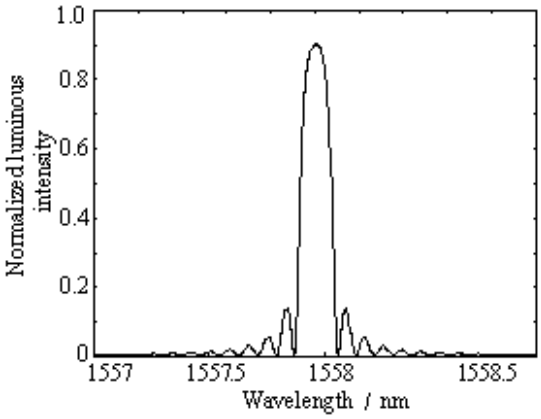

Fig.2 The relationship between LPFG transmission spectrum and bending curvature

Figure 2 shows, with the LPFG bending (curvature) increases, LPFG T_λ enhanced LPFG transmission, the transmission spectrum of the resonant peak amplitude decreased gradually, resonant peak wavelength red shift occurs.

3.2 Circular diaphragm strain characteristics

ISSN: 1992-8645 www.jatit.org E-ISSN: 1817-3195

The edges of the clamping, subjected to uniform pressure p round diaphragm, the low pressure surface at an arbitrary point has a radial stress s_r and a tangential stress s_t [4-5]:

$$s_r = \frac{3pR^2\mu}{8t^2}\left[\left(\frac{1}{\mu}+1\right)-\left(\frac{3}{\mu}+1\right)\left(\frac{r}{R}\right)^2\right] \quad (5)$$

$$s_t = \frac{3pR^2\mu}{8t^2}\left[\left(\frac{1}{\mu}+1\right)-\left(\frac{1}{\mu}+3\right)\left(\frac{r}{R}\right)^2\right] \quad (6)$$

Any point offset (i.e. deflection) is given by:

$$y = \frac{3p\left(1-\mu^2\right)\left(R^2-r^2\right)^2}{16Et^3} \quad \left(0 \le r \le \frac{R}{2}\right) \quad (7)$$

The type (7) an order and two order differential get:

$$y' = \frac{3p\left(1-\mu^2\right)\left(r^3-R^2r\right)}{4Et^3} \quad (8)$$

$$y'' = \frac{3p\left(1-\mu^2\right)R^2}{4Et^3} \quad (9)$$

By the formula (7) shows: when $r=0$, that is at the center, the largest circular diaphragm deflection, and the maximum deflection H:

$$H = y\big|_{r=0} = \frac{3p\left(1-\mu^2\right)R^4}{16Et^3} \quad (10)$$

By type (10) deformation of the pressure and the relationship between H to p:

$$p = \frac{16Et^3H}{3\left(1-\mu^2\right)R^4} \quad (11)$$

According to the curvature equation, and into the type (8), (9) and (11), a circular diaphragm center of curvature C:

$$C\big|_{r=0} = \frac{\left|y''\right|}{\left(1+y'^2\right)^{3/2}} = \frac{3p\left(1-\mu^2\right)R^2}{4Et^3} = \frac{4H}{R^2} \quad (12)$$

Type: H is at the center of the circular diaphragm deflection, i.e. the center deflection (long period fiber grating curvature, unit: m).

Based on the formula the curvature and deflection at the center, C H linearly, coefficient of $4/R^2$. At the same time, the curvature C as long period fiber grating curvature (m-1) and LPFG output spectrum characteristics are associated.

Combined type (1), (2), (3) and (4) available, LPFG resonant transmission spectrum of resonant peak amplitude of A and pressure p relationship:

$$A = f[C(p)] = f[\frac{3(1-\mu^2)pR^2}{4Et^3}] \quad (13)$$

By type (13) that: along with the pressure increasing p, circular diaphragm deflection increases, the center of curvature change, so that the LPFG curvature increases, LPFG resonant wavelength transmission enhancement, the transmission spectrum of the LPFG resonant peak amplitude decreased, resonant wavelength, and the resonant peak amplitude and pressure p linear A relationship.

In addition, the circular diaphragm in the large displacement exhibit nonlinear, stretching function added to the basic bending, thereby creating a stiffening effect. The stress of nonlinear followed the center offset y_c nonlinear, which follows the relationship [5]:

$$p = \frac{16Et^4}{3R^4(1-\mu^2)}\left[\frac{y_c}{t}+0.488\left(\frac{y_c}{t}\right)^3\right] \quad (14)$$

Type: p membrane surface pressure differential, E as the modulus of elasticity for diaphragm thickness, t, μ as Poisson's ratio, as to the clamping edge radius of the diaphragm.

By formula (14) shows, the yc/t design was full of small, which can achieve the desired nonlinear. It is important to note, small yc/t will also bring a small strain.

The above derivation shows, when the circular diaphragm materials, dimensions is given, along with the pressure increasing, at the center of the deflection and curvature change will gradually change from nonlinear to linear.

3.3 Numerical analysis

Using ANSYS 10 software for numerical analysis, selection of circular diaphragm size and material characteristics are as follows: determine the plate radius is RRRR=27.934 mm, a film thickness of t=0.12 mm, stainless steel material, the modulus of elasticity is E =190 GPa, Poisson's ratio is μ=0.305, edge clamped, membrane surface under uniform force FFF, and FFF by 0 added to

Journal of Theoretical and Applied Information Technology
20th April 2013. Vol. 50 No.2

ISSN: 1992-8645 www.jatit.org E-ISSN: 1817-3195

0.25 MPa. Simulation of circular diaphragm at the center of the deflection change with pressure curve as shown in figure 3.

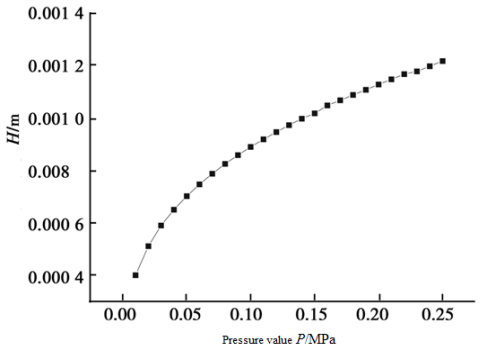

Fig.3 Central deflection of the disk-shape diaphragm

In different atmospheric pressures, according to figure 3 YYY simulation curves, grating curvature with air pressure changes gradually from nonlinear to linear. Due to bending and deflection, resonant peak amplitude and a linear relationship, resonant peak amplitude varies with the gas pressure relationships should also follow the trend. Therefore, using LPFG on the diaphragm microbending sensitivity, by Xie Zhenfeng amplitude change measurement environment pressure value.

4. LPFG PRESSURE SENSOR TEST

4.1 The test system structure

Based on long period fiber grating pressure sensor structure, as shown in figure 4. Test system components include: box film encapsulation structure, LPFG sensing probe and a pressure gauge. Among them, the diaphragm is the pressure sensitive element. Pressure changes when the two sides of the diaphragm, the surface pressure difference, the diaphragm will cause distortion. LPFG sensing probe is stuck on the lower surface of the diaphragm, the diaphragm deformation makes with LPFG resonance peak amplitude change, thus the pressure variation into LPFG resonant peak amplitude variation.

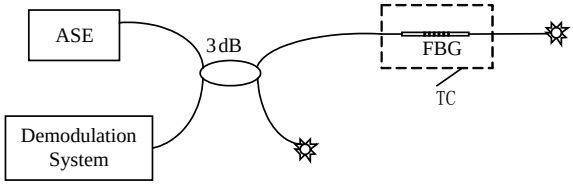

Fig.4 The scheme of the LPFG atmospheric pressure sensor

Based on the strain distribution along the diameter direction, LPFG paste in circular diaphragm near the center. Diaphragm material is stainless steel (0Cr17Ni12Mo2) for 190 GPa, elastic modulus, Poisson's ratio is 0.305, the thickness of 0.12 mm, 55.868 mm in diameter, the experimental device as shown in figure 4. System based on LPFG center wavelength at 1530.153 nm, the length of the grating was 3.75 cm; use a broadband light source (Agilent 83437A) as input, through the AQ6317C spectrum acquisition of long period fiber grating transmission spectrum changes. During the experiment, through the pressure pump (2J-TM-50/40) to the pressure sensor pressure, start with 0.02 MPa, each with 0.01 MPa to do a survey, to 0.25 the end of MPa. For detecting and sensing system repeatability, targeting the same measurement range, repeated compression /decompression measurement [7-11].

4.2 The result of testing and analysis

Figure 5 gives the harmonic amplitude value with the diaphragm by pressure changes in experimental curve, numerical analysis and ANSYS above the trend line. Figure 5 shows along with the change in air pressure, long period fiber grating harmonic amplitude value decreased from 16.712 dB to 6.495 dB, and the change is having good regularity, its response to dB/hPa. Resonance peak wavelength change also has very good regularity. In the pressure range, wavelength of 1.54 nm. Experiments show that, in the repeated /buck process, the pressure sensor can maintain a good repeatability and sensitivity.

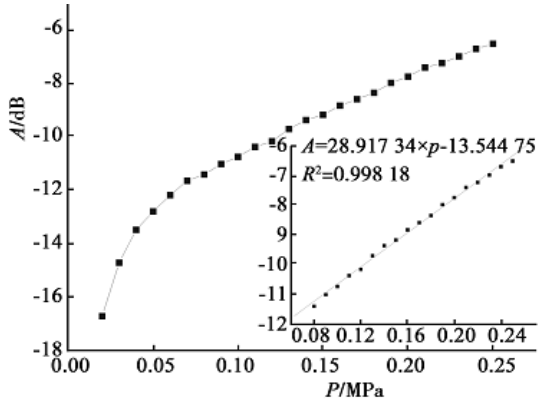

Fig.5 The relationship between LPFG resonance peaking amplitude and atmospheric pressure

LPFG pressure sensor pressure in initial stage is (0.02 ~ 0.07 MPa), because the stiffening effect exhibited nonlinear incremental changes. With the increase of pressure, the resonant amplitude and pressure values (0.07 ~ 0.25 MPa) show a good

ISSN: 1992-8645 www.jatit.org E-ISSN: 1817-3195

linear relationship, the linear fitting equation is: A=28.917 34 P – 13.54475, a correlation coefficient of 0.99818, fitting the standard deviation is 0.09988, as shown in figure 5.

The diaphragm material for copper (Cu) for 119 GPa, elastic modulus, Poisson's ratio is 0.326, the thickness of 0.96 mm, 55.868 mm in diameter, according to the above method is tested by curve, as shown in figure 6. Compared with stainless steel sheet, its higher sensitivity, in 0.12～0.30 MPa within is better, but the initial stage of compression yield stress is affected [12-14].

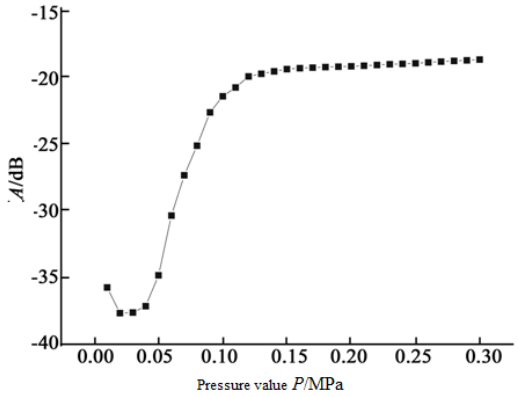

Fig.6 The response curve of a copper membrane

The experiment was found in the grating axial stress influence mainly manifests for the resonant peak wavelength shift amount decreases, that is to say, in the compression process, due to the axial stress increases ceaselessly, resonant peak offset to less than no axial stress condition of offset. Properly reduce the adhesive on the LPFG axial tension, can be made in the free state of LPFG curvature as possible with the diaphragm deflection be consistent.

In addition, the pressure sensor measurement range is determined by the diaphragm thickness and material. If use the elastic modulus and thickness of the film, it will be at the early stage of loading (0.05 MPa) stress yield phase,and the range can be reduced, copper (thickness of 0.96 mm) response curve is shown in figure 6.

5. CONCLUSIONS

Long-period fiber grating (LPFG) has a sensitive characteristic that its resonance spectrum changes with bending curvature. By designing an LPFG-bellows seal structure; we developed a LPFG atmospheric pressure sensor based on bending curvature characteristic resonance peaking modulation. ANSYS numerical analysis and experimental results indicate that when the atmospheric pressure changes from 0.02 MPa to 0.25 MPa, the resonance peaking amplitude falls from 16.712 dB to 6.495 dB and the resonance peaking wavelength is red-shifted about1.54 nm. The resolution is 4.086 8×105 dB/hPa. In the range of atmospheric pressure measured in the experiment, the sensor system has good sensitivity and repeatability, which can satisfy the need of meteorology and flight vehicle monitoring highly.

REFERENCES

[1] WANG L, DU Y, SONG Y Q, et al. Development for gas pressure sensitive materials[J]. Optical Instruments, 2004, 26(2):211-217.

[2] XIAO S R, ZHU P, BEN F L. Analysis on characteristics of optical fiber sensor for atmospheric pressure[J]. Optics and Precision Engineering, 2008,16(6):1042-1047.

[3] RAO Y J, WANG Y P, RAN Z L, et al. Characteristics of novel long-period fiber gratings written by focused high-frequency CO2 laser pulses[J]. Asia-Pacific Optical and Wireless Communications 2001, Proc. SPIE, 2001, 4581:327-333.

[4] ZHAO H X, BAO J L, CHEN Y. Effect of bending curvature on transmission spectra of long period fiber gratings[J]. Chinese Journal of Lasers, 2008,35(5):722- 725.

[5] DOEBELIN E O. Measurement systems application and design[M]. Beijing: Publishing House of Electronics Industry, 2007.

[6] LIU H W. Material mechanics[M]. Beijing: Publishing House of Higher Education,2002.

[7] WANG Y P, RAO Y J, ZENG X K. Bending characteristics analysis of long-period fiber gratings using coupled mode theory[J]. Acta Photonica Sinica, 2002,31(10):1205- 1208.

[8] YANG L, LI G M, KANG L, et al. Signal acquisition for atmospheric pressure transducer based on multi-period measurement[J]. Chinese Journal of Scientific Instrument, 2007,28(4):687-691.

[9] WANG Y, LIANG D K, ZHOU B. Vibration monitoring of smart structure using micro-bending characteristic of long-period fiber grating[J]. Chinese Journal of Scientific Instrument, 2008,29(6):1154-1158.

[10] XIAO SH R, CHANG J H, BEN F L. Multi-path optical fiber sensor for atmospheric pressure[J]. SPIE, 2007, 6836: 68361G-1-6.

ISSN: 1992-8645 www.jatit.org E-ISSN: 1817-3195

[11] Zhou Zhi, Wu Zhanjun, Tian Shizhu, et al, "Studies on properties of temperature sensing for optical fiber FBGs," Piezoelectric & Acousto-optic, 24(6), 2002, pp.430-433.

[12] Zhang Song and Zhang Jin-ping, "Study on FBG demodulator based on single-chip microcontroller system," China Measurement&Test ,Vol.35 No.6, November ,2009, pp.220-350.

[13] Y. Zhao and Y. Liao, "Discrimination methods and demodulation techniques for fiber Bragg grating sensors," Optics and Lasers in Engineering,Vol.41. 1-18, 2004.

[14] Zhang Guoping, "Design of Portable Vibration Monitoring System Based on Wavelet Theory," Modern Machinery, March， 2010, Vol.20, pp.28-30.